Eur. J. Biochem. *256*, 580−588 (1998)

Uracil DNA glycosylase from *Mycobacterium smegmatis* and its distinct biochemical properties

Kedar PURNAPATRE and Umesh VARSHNEY

Department of Microbiology and Cell Biology, Indian Institute of Science, Bangalore, India

(Received 14 April/18 June 1998) − EJB 98 0503/4

Deamination of cytosine residues contributes to the appearance of uracil in DNA. Uracil DNA glycosylase (UDG) initiates uracil excision repair to safeguard the genomic integrity. To study the mechanism of uracil excision in mycobacteria (organisms with G+C rich genomes), we have purified UDG from *Mycobacterium smegmatis* by more than 3000-fold. The molecular mass of *M. smegmatis* UDG, as determined by SDS/PAGE, is ≈25 kDa and it shows maximum activity at pH 8.0. The N-terminal sequence analysis shows that the initiating amino acid, formyl-methionine is cleaved from the mature protein. More interestingly, unlike *Escherichia coli* UDG, which forms a physiologically irreversible complex with the inhibitor protein Ugi, *M. smegmatis* UDG forms a dissociable complex with it. *M. smegmatis* UDG excises uracil from the 5′-terminal position of the 5′-phosphorylated substrates. However, its excision from the 3′-penultimate position is extremely poor. Similar to *E. coli* UDG, *M. smegmatis* UDG also uses pd(UN)p as its minimal substrate. However, in contrast to *E. coli* UDG, which excises uracil from different loop positions of tetraloop hairpin substrates with highly variable efficiencies, *M. smegmatis* UDG excises the same uracil residues with comparable efficiencies. Kinetic parameters (K_m and V_{max}) for uracil release from synthetic substrates suggest that *M. smegmatis* UDG is an efficient enzyme and better suited for molecular biology applications. We discuss the usefulness of the distinct biochemical properties of *M. smegmatis* UDG in the possible design of selective inhibitors against it.

Keywords: UDG; Ung; Ugi; hairpins; mycobacteria.

Mycobacteria are responsible for a variety of public health problems. According to the recent WHO reports, a third of the world population is infected with *Myobaceterium tuberculosis*, and approximately 30 million deaths are likely to occur in the next 10 years on account of tuberculosis. Further, the emergence of drug-resistant strains has made it imperative to understand the biology of these organisms [1, 2]. Mycobacteria multiply inside the host macrophages where they are exposed to oxidative or other physiological stresses [2−5]. Such adverse conditions result in damage to DNA [6, 7]. However, the mechanisms of DNA repair in these important organisms have not been investigated so far. Mycobacteria are at increased risk of cytosine deamination not only because of their G+C-rich genomes (up to 70%) but also because of the unfavorable habitat of the host macrophages where they multiply. Deamination of cytosine residues results in the appearance of uracil residues in DNA, which, unless repaired, lead to G:C→A:T mutations.

Uracil DNA glycosylase (UDG) is responsible for uracil excision repair and crucial in safeguarding the genomic integrity [8−11]. UDGs characterized so far require no metal ions or other cofactors for their activity and can be divided into two groups. A number of diverse proteins such as the cyclin-like UDG [12], dsUDG [13] and other proteins such as glyceraldehyde-3-phosphate dehydrogenase [14] can be classified into one group. The other group consists of UDGs which show striking similarity in their sequences and three-dimensional structures [15−19].

We are interested in the mechanism of uracil excision repair in mycobacteria. In this study, we describe the purification and characterization of UDG from *M. smegmatis*.

MATERIALS AND METHODS

Bacterial strains, growth media and plasmids. *Mycobacterium smegmatis SN2*, a laboratory strain was grown in YK medium [20] to late log phase (28 h). *Escherichia coli* TG1 (Amersham) was grown in 2YT medium in the presence of 100 μg ml^{-1} ampicillin [21] and used as a host for overexpression of *E. coli* UDG [22] and the *Bacillus subtilis* phage, PBS-2-encoded uracil DNA glycosylase inhibitor, Ugi [23]. pTrc99C and pKK233 (Pharmacia) were used as expression vectors for *E. coli* UDG and Ugi, respectively. *Bacillus subtilis* strains carrying phage PBS-2 were kind gifts from Drs I. Takahashi and H. E. Schellhorn (McMaster University, Hamilton, Canada) and M. Williams (The Ohio State University, Columbus, USA).

Labeling of oligodeoxyribonucleotides (oligonucleotides). Oligonucleotides were purified, quantified and made up to a final concentration of 10 pmol μl^{-1} [24, 25]. Oligonucleotides (10 pmol) were 5′ end labeled with 20 μCi of [γ-^{32}P]ATP (3000 Ci $mmol^{-1}$) and T4 polynucleotide kinase, and purified on Sephadex G-50 minicolumns.

UDG assays. *Genomic DNA degradation assay. E. coli* RZ1032 (*dut1 ung1*) genomic DNA (1 μg) was incubated with

Correspondence to U. Varshney, Department of Microbiology and Cell Biology, Indian Institute of Science, Bangalore, 560 012, India

Fax: +91 80 334 1683.

E-mail: varshney@cge.iisc.ernet.in

Abbreviations. UDG, uracil DNA glycosylase; Ugi, uracil DNA glycosylase inhibitor protein.

Enzyme. Uracil DNA glycosylase (EC 3.2.2.3).

protein extracts in 15-μl reactions consisting of 1×UDG buffer (50 mM Tris/HCl, pH 8.0, 1 mM Na_2EDTA, 1 mM dithiothreitol and 25 μg ml^{-1} BSA) for 10 min, mixed with an equal volume of 0.1 M NaOH, heated at 90 °C for 10 min and analyzed on 1% agarose gels containing 0.5 μg ml^{-1} ethidium bromide using TBE buffer system [21]. Fast mobility DNA fragments (smear) corresponded to high UDG activity.

Oligonucleotide degradation assay. 5′ end labeled, dUMP containing oligonucleotides (1 pmol) were treated with UDG in 15-μl reactions containing 1×UDG buffer, incubated at 37 °C for 10 min, mixed with equal volume of 0.1 M NaOH, heated at 90 °C for 10 min, dried in a speed vac, taken up in 10 μl formamide dye and analyzed on 15% polyacrylamide/8 M urea gels [21]. The substrate (S) and the product (P) bands were visualized by autoradiography.

Enzyme activities (Table 1) were determined by mixing *E. coli* RZ1032 (*dut1 ung1*) genomic DNA (0.5 μg) with the assay mixtures containing 1 pmol 5′ end labeled oligonucleotide having dUMP in its fourth position (SS-U4, 24), and the bands corresponding to substrate and product arising from the oligonucleotide were cut out of the gel and quantified. The percent uracil excision was calculated as 100×[P/(S+P)].

Post end-labeling UDG reaction. Oligonucleotides (0.5 pmol) were reacted with UDG in 15-μl volumes and heated in the presence of 0.1 M NaOH as described above and supplemented with equivalent amounts of 0.1 M HCl. Aliquots (2 μl) from the reaction were then either treated or not treated with calf intestinal alkaline phosphatase [25] and subjected to 5′ end labeling reaction with T4 polynucleotide kinase (1 U) in the presence of 10 μCi [γ-^{32}P]ATP. The products were electrophoresed on 15% or 18% polyacrylamide 8 M urea gels [21] and visualized by autoradiography.

Purification of UDG from *M. smegmatis*. All steps were carried out at 4 °C and UDG activity was monitored by the genomic DNA degradation assay. The cell pellet (110 g, wet mass) was suspended in 80 ml 20 mM potassium phosphate, pH 7.4, 10% glycerol (by vol.), sonicated three times for 5 min each at 50% duty cycles and a pulse time of 5 s with 3 min gaps inbetween successive cycles of sonication, and clarified by centrifugation. The supernatant was further centrifuged at 100 000 *g* for 2 h and the S-100 supernatant (fraction I) was loaded onto a DEAE-Sephacel (Sigma) column (2.2 cm×29 cm). The column was washed with 250 ml loading buffer [20 mM potassium phosphate, 10% glycerol (by vol.), pH 7.4] and eluted with 400 ml buffer by applying salt and pH gradients (20 mM potassium phosphate, pH 7.4, to 500 mM potassium phosphate, pH 6.8). UDG eluted at ≈220−320 mM potassium phosphate. The enriched fractions were pooled and the proteins were precipitated by adding solid ammonium sulfate to 70% saturation and recovered by centrifugation. The pellet was solublized in 7.5 ml buffer (10 mM Hepes, pH 7.4, 1 M NaCl; fraction II) and chromatographed on a Sephadex G-75 (Pharmacia) column (3 cm×80 cm). Fractions enriched in UDG were pooled and subjected to 70% ammonium sulfate saturation. The precipitate was recovered and dissolved in 17 ml 50 mM Hepes, pH 7.4, dialyzed against the same buffer and the dialyzed proteins (fraction III) were loaded onto a 5 ml Mono-S column (High-S column, BioRad) and eluted with 50 ml Hepes, pH 7.4, with 0−1 M NaCl. UDG eluted at ≈300 mM NaCl and the enriched fractions were pooled, dialyzed against 500 ml 20 mM Tris/HCl, pH 7.4, 10% glycerol (by vol.) and the contents (fraction IV) were loaded on to a ssDNA-agarose (Gibco-BRL) column (1.5 cm×7 cm). The column was washed with 15 ml loading buffer and eluted with 20 ml of the same buffer in the presence of 0−1 M NaCl. UDG eluted at ≈400 mM NaCl. The active fractions were pooled and dialyzed twice against 5 mM potassium phosphate, pH 7.5. The dialyzed sample (fraction V) was then loaded on to hydroxyapatite column (1.3 cm×3.5 cm, Bio-Rad) and the column was washed with 10 ml loading buffer. UDG was eluted by applying a 12-ml gradient of 5−100 mM potassium phosphate, pH 7.5. UDG eluted at ≈50 mM potassium phosphate. The active fractions were pooled and dialyzed against 20 mM Tris/HCl, 50 mM NaCl, 1 mM dithiothreitol, 1 mM Na_2EDTA and 50% glycerol (by vol.) and stored (fraction VI).

Purification of *E. coli* UDG and phage PBS-2 encoded inhibitor protein, Ugi. *E. coli* UDG was purified as described [24, 26]. Ugi gene was PCR amplified from PBS-2 DNA, cloned into pTZ18R, confirmed by sequencing and subcloned into pKK233. Ugi was purified [23] and stored in 20 mM Tris/HCl, 100 mM NaCl and 50% glycerol (by vol.).

Electroelution and assay of *M. smegmatis* UDG activity. Fraction VI was electrophoresed in two adjacent lanes (0.5 μg $lane^{-1}$) on a 15% SDS/PAGE [27] and one of the lanes was sliced into seven pieces using stained molecular-mass size markers (BioRad) as reference. The individual gel pieces were placed into dialysis bags containing 1 ml 20 mM Tris/HCl, pH 8.0 and electroeluted using a mini gel tank filled with the same buffer, for 3 h at 150 V. The bags were then removed and dialyzed against 20 mM Tris/HCl, pH 8.0, 1 mM Na_2EDTA and 1 mM dithiothreitol. Aliquots (20 μl) were assayed for UDG activity. The gel corresponding to the other lane was stained with Coomassie blue to locate the protein band. In another experiment, the 25-kDa band was precisely cut from a Coomassie-blue-stained gel, boiled in sample loading buffer [50 mM Tris/HCl, pH 6.8, 100 mM 2-mercaptoethanol, 2% SDS, 10% glycerol (by vol.) and 0.01% bromophenol blue (mass/vol.)] for 10 min and re-electrophoresed on 15% SDS/PAGE. The rest of the procedure for electroelution and UDG activity assay was the same as described above.

N-terminal amino acid sequence analysis of *M. smegmatis* UDG. Fraction VI (5 μg) was electrophoresed on 15% SDS/PAGE, electroblotted to a poly(vinylidene difluoride) membrane [28] and stained with Ponceau dye. Only one band (≈25 kDa) was detected. The band was cut out, washed thoroughly with several changes of water and submitted for N-terminal sequence analysis at the microsequencing facilities at Massachusetts Institute of Technology (Cambridge, USA) and Indian Institute of Science (Bangalore, India).

Determination of pH optima. UDG reactions were performed using a 27-residue oligonucleotide containing dUMP at the fourth position, as substrate (1 pmol) in the various buffers of 50 mM strength. All buffers were supplemented with 1 mM Na_2EDTA, 1 mM dithiothreitol and 25 μg ml^{-1} BSA. The pH of the various buffers were as follows: citrate phosphate, pH 6.5; Mops, pH 7; Tris/HCl, pH 7.5, 8.0, 8.5 and 9.0; sodium carbonate/bicarbonate, pH 9.5.

Interaction of UDG with Ugi. UDG (20 pmol) from *E. coli* or *M. smegmatis* (fraction VI) was incubated with 10, 20 or 30 pmol Ugi in the presence of 20 mM Tris/HCl, pH 8.0, in a 20-μl reaction at 25 °C for 20 min and stored on ice for 20 min. Aliquots (2 μl) were assayed for UDG activity and the remainder of the contents analyzed on a 7−18% native PAGE. The proteins were visualized by Commassie brilliant blue staining.

Elution of UDG-Ugi complex. The native gels used to fractionate UDG-Ugi complexes were sliced from top to bottom into eight parts and the pieces transferred to 1.5-ml Eppendorf tubes containing 0.5 ml 20 mM Tris/HCl, pH 7.4, 1 mM Na_2EDTA. Diffusion of the proteins into the buffer was facilitated by gently shaking the tubes on a rocking platform for 2 h at room temperature. Aliquots (20 μl) were used for UDG assays.

Table 1. Purification scheme. 1 unit is the amount of protein required to excise 1% uracil from a 15-µl reaction containing 1 pmol 5′ ^{32}P-labeled synthetic DNA and 0.5 µg genomic DNA of *E. coli* RZ1032 (*dut1 ung1*) in 10 min at 37°C.

Fraction	Volume	Total activity	Total protein	Specific activity	Purification
	ml	Units	mg	Units mg^{-1} total protein^{-1}	-fold
Fraction I (S-100)	160	16960	3712	4.5	1
Fraction II (DEAE-Sephacel)	7.5	3900	289.5	13.5	3
Fraction III (Sephadex G75)	17	2856	40.3	71	16
Fraction IV(Mono-S)	42	1218	3.6	338	75
Fraction V (DNA-agarose)	5	937.5	0.95	986.8	219
Fraction VI (Hydroxyapatite)	3.5	700	0.05	14000	3111

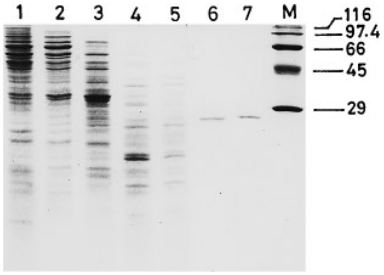

Fig. 1. Purification of UDG from *M. smegmatis*. A representative SDS/PAGE (15%) showing protein profile of fractions I−IV. Lane 1, S-100 extract (fraction 1, 10 µg); lane 2, DEAE-Sephacel pool (fraction II, 4.7 µg); lane 3, Sephadex G-75 pool (fraction III, 3 µg); lane 4, Mono-S pool (fraction IV, 2 µg); lane 5, SS-DNA agarose pool (fraction V, ≈2 µg); lane 6, hydroxyapatite pool (fraction VI, 0.25 µg); lane 7, *E. coli* UDG (0.25 µg); lane 8, molecular-mass standards; *β*-galactosidase (116 kDa), phosphorylase *b* (97.4 kDa), bovine serum albumin (66 kDa), ovalbumin (45 kDa) and carbonic anhydrase (29 kDa).

Preparation of pd(UT)p. 5′ ^{32}P end-labeled pd(UTA) was depurinated in 0.4 M HCl for 20 h at 37°C and neutralized with NaOH. The reactions were then further supplemented with 0.1 M NaOH and heated at 90°C for 30 min to generate pd(UT)p. The labeled pd(UTA) and pd(UT)p were recovered from 18% native PAGE by elution in 20 mM Tris/HCl, pH 7.4, and purified on Sep-pak (Millipore) minicolumns.

Determination of K_m and V_{max} values. The radiolabeled oligonucleotides were mixed with the corresponding unlabeled oligonucleotides such that the contribution from the labeled counterpart was much less than 1%. For K_m and V_{max} determinations, 15 µl reactions containing various substrate concentrations were carried out using appropriate dilutions of UDG (fraction VI). K_m and V_{max} values were determined as described [29].

Protein estimations. Proteins were estimated by modified Bradford's assay [30] using BSA as a standard. Compared to the values obtained using the absorption coefficient, this method underestimates *E. coli* UDG by approximately 10%. Ugi was estimated by its absorbance at A_{280} ($\varepsilon_{280\ nm} = 1.2\times10^4$).

RESULTS

Purification of *M. smegmatis* UDG. UDG was purified 3111-fold with a recovery of 4.2% (Table 1). The specific activity of the hydroxyapatite elute was the highest and it showed a single protein band of 25 kDa suggesting it to be *M. smegmatis* UDG (Fig. 1). It was also seen that *M. smegmatis* UDG is of approximately the same size as *E. coli* UDG (compare lanes 6 and 7). Using a synthetic single-stranded substrate (SS-U9), the specific activity of fraction VI was 226 pmol min^{-1} ng^{-1} (Table 3).

Electroelution of the 25 kDa protein and assay of UDG activity. To confirm that the 25-kDa protein in fraction VI was responsible for UDG activity, gel pieces from SDS/PAGE corresponding to different molecular-size regions were electroeluted and assayed for UDG activity. Only the eluate from the gel piece that contained the 25-kDa band showed UDG activity (Fig. 2A, B). To further confirm this result, the 25-kDa band was precisely cut out of a Coomassie-brilliant-blue-stained gel, re-fractionated by SDS/PAGE and electroeluted. In this experiment too, the UDG activity eluted with the gel piece that contained the 25-kDa region (Fig. 2C, lane 2). Not unexpectedly though, the UDG activity was not as pronounced as in Fig. 2B (lane 2). Nevertheless, these experiments provided strong evidence that the 25-kDa band indeed corresponds to *M. smegmatis* UDG.

N-terminal sequence analysis. Microsequence analysis showed TARPLNELVE as the N-terminal sequence of *M. smegmatis* UDG. The N-terminal begins with a threonine residue and suggests post-translational removal of the initiating amino acid, formyl-methionine.

pH optima of *M. smegmatis* UDG. *M. smegmatis* UDG showed maximum activity at pH 8 (Fig. 3). Interestingly, the activity profile also suggested another broad pH optima at pH 8.5−9.0.

Interaction of *M. smegmatis* UDG with Ugi. Ugi inhibits UDG by forming an inactive UDG-Ugi complex in 1:1 molar stoichiometry. The complex of *E. coli* UDG with Ugi is exceptionally stable and it does not exchange with free Ugi [31, 32]. To study the UDG-Ugi interaction, 20 pmol *M. smegmatis* UDG (or *E. coli* UDG as a control) was mixed with 10, 20 or 30 pmol Ugi in a 20-µl volume. Protein-protein interactions were analyzed by electrophoresis of 18 µl of the mix on a 7−18% native polyacrylamide gel (Fig. 4B). Under the conditions used, UDG from both the sources migrated in the form of a smear which was not detected by Coomassie brilliant blue staining. However, Ugi, a highly acidic protein (pI 4.2) of low molecular mass, migrated as a sharp band (Fig. 4B, lane 9). As expected for *E. coli* UDG, there was a near quantitative increase in the amount of the complex formed when Ugi levels were increased from 10 pmol to 20 pmol (Fig. 4B, lanes 2 and 3). A band corresponding to free Ugi was seen only when it was added at 1.5 molar excess (Fig. 4B, lane 4). In contrast, only a small fraction of *M. smegmatis* UDG was seen in the complex even at 1.5 molar excess of Ugi (Fig. 4B, lane 8). In fact, the free Ugi band was detectable even at a substoichiometric molar ratio of 0.5 (Fig. 4B, lane 6) and its intensity increased in the lanes with increased levels of Ugi (1:1, lane 7 or 1:1.5, lane 8). When equal amounts of *E. coli* and *M. smegmatis* UDGs were analyzed on SDS/PAGE (Fig. 4C), they showed equal band intensities upon Coomassie brilliant blue staining, suggesting that the low level of complex formation with *M. smegmatis* UDG could not be due to its over-

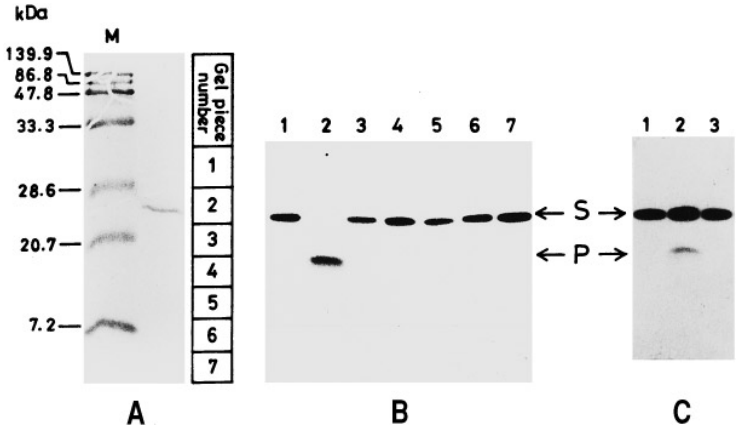

Fig. 2. Electroelution of the 25-kDa protein (*M. smegmatis* UDG) and activity assays. (A) *M. smegmatis* UDG was fractionated by SDS/PAGE into two lanes (0.5 μg lane^{-1}) adjacent to stained protein molecular-mass (M_r) standards (BioRad). Gel corresponding to one of the UDG lanes was sliced as shown into seven pieces and subjected to electroelution, and the remaining gel was stained with Coomassie brilliant blue. (B) UDG assays using eluates from gel pieces 1−7. (C) The 25-kDa protein band from a Coomassie brilliant blue stained SDS/PAGE was cut out and the solublized protein fractionated by SDS/PAGE and electroeluted as in (A). UDG assays with the eluates from the first three gel pieces are shown in lanes 1−3. Bands marked, S and P correspond to the substrate and the products.

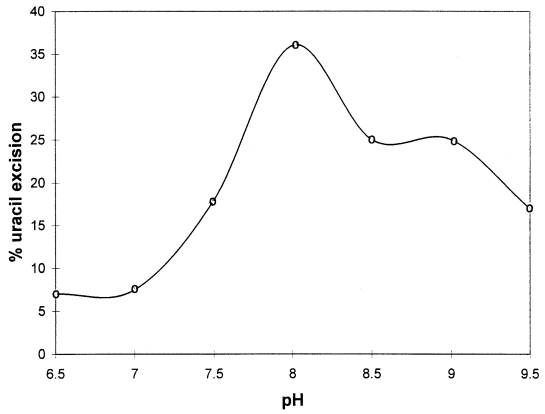

Fig. 3. pH optima of *M. smegmatis* UDG. Standard assays in the buffers of varying pH were used to determine the uracil excision.

estimation. Furthermore, to rule out that the low level of complex formation was not a result of inactivation of *M. smegmatis* UDG preparation either, enzyme assays were performed on the remaining 2-μl aliquots from each of the mixes (Fig. 4A). As expected, complete inhibition of *E. coli* UDG was observed at the equimolar concentration of Ugi (Fig. 4A, compare lanes 2 and 4). In contrast, inhibition of *M. smegmatis* UDG was not complete even at a 1.5-molar excess of Ugi (Fig. 4A, compare lanes 6 and 9). These observations, therefore, suggested a weak interaction of Ugi with *M. smegmatis* UDG.

Elution of UDG-Ugi complexes and UDG assays. To further establish that the interaction of *M. smegmatis* UDG with Ugi was indeed weak, complexes of *E. coli* or *M. smegmatis* UDGs with Ugi formed in the presence of a twofold molar excess of the latter were fractionated on the native polyacrylamide gel (Fig. 4B). Proteins from the various regions of the gel were allowed to diffuse into the elution buffer (Materials and Methods) and assayed for UDG activity. As expected for an undissociable complex, eluates from the gel piece(s) corresponding to *E. coli* UDG-Ugi complex did not show appreciable UDG activity (Fig. 5A). However, the eluates from the gel pieces corresponding to *M. smegmatis* UDG-Ugi complex showed substantial UDG activity (Fig. 5B, lanes 5 and 6). The observation that the gel pieces 2, 3 and 4 also showed some activity (Fig. 5B, lanes 2, 3 and 4), suggested that the *M. smegmatis* UDG-Ugi complex dissociated even as it migrated into the gel. These experiments confirmed that *M. smegmatis* UDG forms a dissociable complex with Ugi.

Substrate specificities. The observation that *M. smegmatis* UDG formed a dissociable complex with Ugi, suggested that it is distinct from *E. coli* UDG. Hence, in the following experiments, a number of dUMP-containing oligonucleotides (Table 2) were used to determine the substrate specificities of *M. smegmatis* UDG.

Excision of uracil from the 5′ ends of DNA oligomers. Excision of 5′ terminal uracil from the substrates generates two radioactively labeled products, sugar-phosphate (Sugar-P_i) and phosphate (P_i) [25]. Oligomers, pd(UTT), pd(UTTT) and pd(UTTTT) produced the two expected products, P_i and sugar-P_i (Fig. 6, lanes 5, 7 and 9, respectively). However, no cleavage products were seen from pd(UT), (compare Fig. 6, lanes 2 and 3) suggesting the minimum substrate size to be more than a dimer for excision of the 5′ terminally located uracil.

Requirement of 5′-phosphate for excision of 5′-terminally located uracil. UDG reactions were performed on the 5′-unphosphorylated (OH) DNA oligomers and the reaction products were detected by the post end labeling method. The size of d(UTTTT) remained unchanged upon treatment with UDG [Fig. 7A, lanes 1−3; owing to the method of detection, the band is indicated as pd(UTTTT)] suggesting that the uracil residue from the 5′ terminal position was not excised in the absence of the 5′ phosphate group. However, when pd(TUTT) was used, a band corresponding to pdTp was seen upon 5′ ^{32}P end labeling of the reaction products (Fig. 7B, lane 2). Under these conditions, detection of the 3′-side-cleavage product [$pd(TT)_{OH}$] was not expected as it contained the nonradioactive 5′-phosphate [25]. A band corresponding to $pd(TT)_{OH}$ was, however, detected when end-labeling was performed subsequent to alkaline phosphatase treatment of the reaction products (Fig. 7B, lane 3). Under these conditions, the 5′ side cleavage product [pd(T)p] could not be detected because the alkaline phosphatase treatment converts d(T)p to $d(T)_{OH}$, which is no longer a substrate for T4 polynucleotide kinase [25].

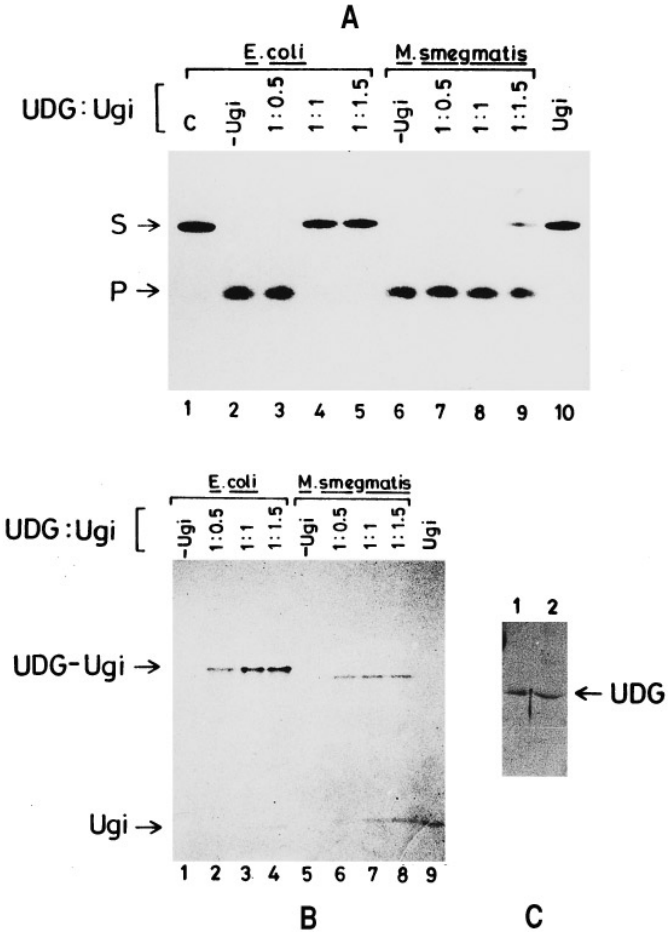

Fig. 4. Interaction of *E. coli* and *M. smegmatis* UDGs with Ugi. UDGs (20 pmol) were incubated alone (-Ugi), or as indicated above the lanes, with Ugi in different molar ratios of 1:0.5, 1:1 or 1:1.5 (10, 20 or 30 pmol Ugi, respectively) in 20-µl volumes. (A) 2 µl aliquots assayed for UDG activity by oligonucleotide degradation method. Lane 1, neither UDG nor Ugi added; lane 10, Ugi (30 pmol); Lanes 2−5 correspond to UDG from *E. coli*, and lanes 6−9 correspond to UDG from *M. smegmatis*. S and P on the left indicate substrate and product bands, respectively. (B) Detection of UDG-Ugi complex (using the remaining 18-µl volumes) by its fractionation on 7−18% native PAGE and staining with Coomassie brilliant blue. Lanes 1−9 correspond to the lanes 2−10 of (A), respectively. (C) Ec- and Ms-UDGs (20 pmol each) fractionated by 15% SDS/PAGE and stained with Coomassie brilliant blue.

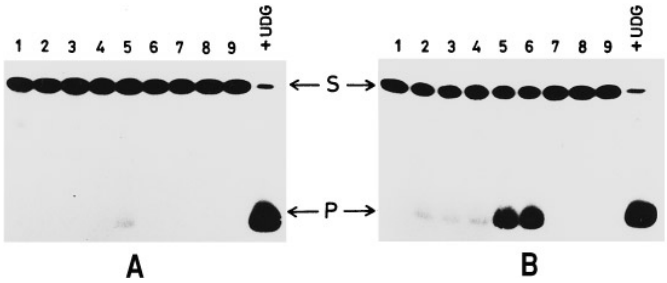

Fig. 5. Electroelution of UDG-Ugi complex. UDG-Ugi complexes were formed and eluted from native gels as described in Materials and Methods. UDG assays from the gel eluates corresponding to *E. coli* UDG-Ugi, and *M. smegmatis* UDG-Ugi are shown in (A), and (B), respectively. Lane 1, substrate alone; lanes 2−9, gel piece numbers 1−8; +UDG, positive controls with *E. coli* and *M. smegmatis* UDGs. S and P indicate the substrate and product bands.

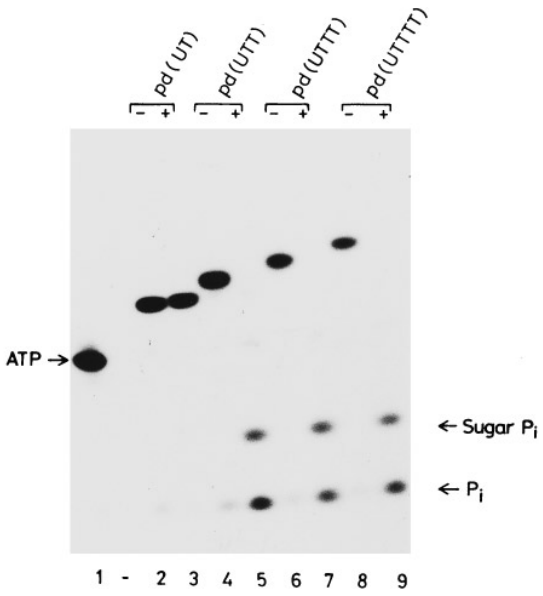

Fig. 6. Excision of uracil from the 5′ position. The 5′ ^{32}P-end labeled DNA oligomers (10 000 cpm) as shown on top of the figure, were either not mixed (−) or mixed (+) with 1 pmol *M. smegmatis* UDG and analyzed by the oligonucleotide degradation assay. Bands marked P_i and sugar-P_i correspond to the products.

Excision of uracil from the penultimate position. Use of pd(TUT), pd(TTUT) and pd(TTTUG) as substrates for *E. coli* or *M. smegmatis* UDGs is shown in Fig. 8. Uracil was not excised from pd(TUT) by either of the enzymes (Fig. 8, lanes 2−4). A detectable release of uracil was seen from pd(TTUT) and pd(TTTUG) by *M. smegmatis* UDG at 1 pmol level of the enzyme [Fig. 8, lanes 7 and 10, respectively; products marked as pd(TT)p and pd(TTT)p]. However, the same substrates, even at fourfold higher (4 pmol) concentration of *E. coli* UDG, produced only barely perceptible signals corresponding to the products. In contrast, a tetrameric substrate pd(TUTT) containing uracil in the third position from the 3′ end was used efficiently by both the *E. coli* and *M. smegmatis* UDGs (Fig. 8, lanes 11−13). Thus, the poor release of uracil from pd(TTUT) and pd(TTTUG) was not because of their small sizes but was a consequence of the location of the uracil residue from the 3′ end.

Minimum substrate size requirement of *M. smegmatis* UDG. Data in Figs 6−8 showed that, (a) a trimeric oligonucleotide pd(UTT) is a substrate for UDG, (b) 5′-end phosphorylation is required for the excision of the 5′-terminally located uracil and, (c) efficient excision of uracil occurred only when its location was moved further in from the second position from the 3′ end. These results suggest pd(UNN) to be the minimum substrate. To further define the minimum substrate size, use was made of yet another oligonucleotide, pd(UTA), to derive pd(UT)p (Materials and Methods). Upon treatment of these oligonucleotides with *M. smegmatis* UDG (Fig. 9), $^{32}P_i$-sugar and $^{32}P_i$ products were seen from pd(UTA) and pd(UT)p (Fig. 9, lanes 3 and 5, respectively) suggesting pd(UT)p to be the minimum substrate for *M. smegmatis* UDG. Oligonucleotide, pd(UT) which is not a substrate for *M. smegmatis* UDG (Fig. 6) was used here as a size marker. Expectedly, pd(UT)p, migrates faster than pd(UT) because of an extra phosphate at the 3′ end.

Uracil release from different positions of tetraloop hairpins. It was recently shown that *E. coli* UDG excised uracil residues from the different positions of tetraloop hairpin substrates with highly variable efficiencies [24]. Fig. 10 A shows the results of

Table 2. List of oligodeoxyribonucleotides.

S.N.	Name	Sequence(5′ to 3′)	Size (nucleoticles)	Remarks
1	SS-U9	d(ctcaagtgUaggcatgcaagagct)	24	U in position 9
2	Loop-U1	d(ctagaggatccUtttggatcct)	22	U in position 1 of tetra loop
3	Loop-U2	d(ctagaggatcctUttggatcct)	22	U in position 2 of tetra loop
4	Loop-U3	d(ctagaggatcctt Utggatcct)	22	U in position 3 of tetra loop
5	Loop-U4	d(ctagaggatcctttUggatcct)	22	U in position 4 of tetra loop
6	Loop-Utcg	d(tggacUtcggtcc)	13	U in position 1 of tetra loop
7	Loop-UUcg	d(tggacUUcggtcc)	13	U in position 1 and 2 of tetra loop
8	Loop-tUcg	d(tggactUcggtcc)	13	U in position 2 of tetra loop
9		d(Ut)	2	U at the 5′ end
10		d(Utt)	3	U at the 5′ end
11		d(Uttt)	4	U at the 5′ end
12		d(Utttt)	5	U at the 5′ end
13		d(tUt)	3	U in position 2
14		d(tUtt)	4	U in position 2
15		d(ttUt)	4	U in penultimate position
16		d(tttUg)	5	U in penultimate position
17		d(Uta)	3	U at the 5′ end

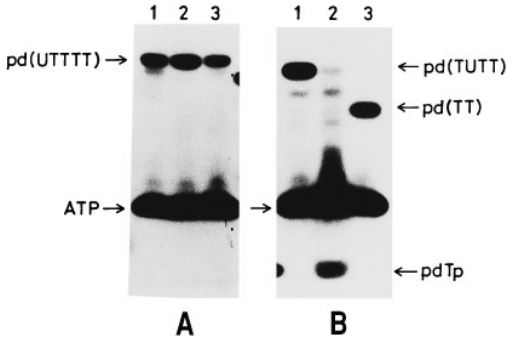

Fig. 7. Requirement of 5′ phosphate for the excision of 5′-terminally located uracil. Oligomers d(UTTTT) (A), or d(TUTT) (B) were reacted with *M. smegmatis* UDG and the products analyzed by 5′ post- end labeling method, with (lanes 3) or without (lanes 2) prior treatment with calf intestinal alkaline phosphatase. Lanes 1 in (A) and (B) are control where the substrates were 5′-end labeled and loaded with no further treatments. The bands corresponding to the substrates and products, as detected by post- end labeling method are as indicated.

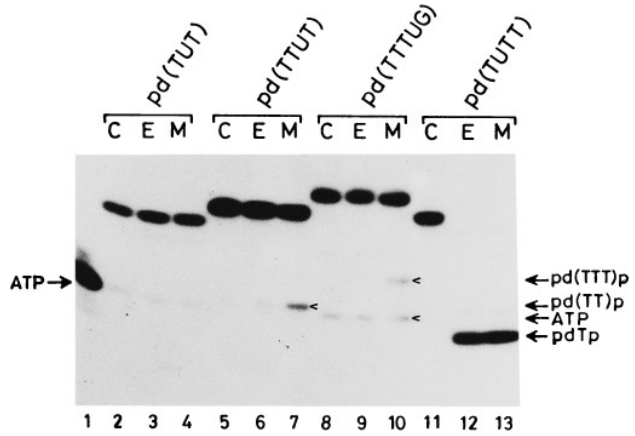

Fig. 8. Excision of uracil from DNA oligomers containing uracil in different positions. 5′-end labeled oligonucleotides (10 000 cpm) were mixed with either 1 pmol *M. smegmatis* UDG (M) or 4 pmol *E. coli* UDG (E) and the reaction products analyzed as shown. (C) Control reactions without UDG.

a range finding experiment using *M. smegmatis* UDG to excise uracil from the first, second, third and the fourth positions of tetra T loops. At 10 fmol *M. smegmatis* UDG, uracil excision from all four substrates was total (Fig. 10 A, lanes 2, 6, 10 and 14) and the relative efficiency of uracil release could not be compared. However, at 1 fmol and 0.1 fmol levels of the enzyme, comparable level of uracil release was seen from all four positions of the tetraloops (Fig. 10 A, compare lanes 3, 7, 11 and 15 or 4, 8, 12 and 16). These results are in sharp contrast with those reported for *E. coli* UDG where the efficiency of uracil release from these substrates varied by more than two orders of magnitude [24]. Use of an another set of tetraloop substrates (Fig. 10 B) showed that the efficient release of uracil from loop regions by *M. smegmatis* UDG was independent of the loop sequence (Fig. 10 A, compare lanes 4, 9 and 14). Interestingly, with loop-UUCG, even at low enzyme concentration (0.1 fmol, Fig. 10 A, lane 9), only a single product was detected corresponding to cleavage at the first position of the loop. Considering that *M. smegmatis* UDG excised uracil from different loop positions at comparable rates, it indicated a processive nature of *M. smegmatis* UDG at least for the excision of neighboring uracils.

For better assessment of the efficiency of uracil release from the tetra T loops, K_m and V_{max} values were determined (Table 3). SS-U9 was used as a reference unstructured substrate. In the case of *M. smegmatis* UDG, both the K_m (0.425−1.05 μM) and the V_{max} (81.9−151.2 pmol min^{-1} ng^{-1}) for the four-loop substrates vary by about twofold, such that the relative efficiency (V_{max}/K_m) of uracil release differed by approximately threefold. This is in marked contrast to the kinetic parameters of *E. coli* UDG which show more than 180-fold difference. A difference in the efficiencies of uracil excision of up to ≈350-fold between the unstructured (SS-U9) and the loop substrates by *E. coli* UDG is also evident (Table 3). Interestingly, this difference, in the case of *M. smegmatis* UDG, is only about fivefold. These results suggest that *M. smegmatis* UDG is more efficient than *E. coli* UDG and should be better suited for the various applications of UDG [33].

DISCUSSION

We have purified UDG from *M. smegmatis* to apparent homogeneity and studied its biochemical properties. At least two

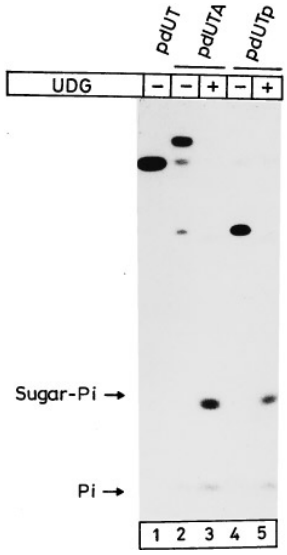

Fig. 9. Minimum substrate for UDG. The 5′-end labeled pd(UTA) and pd(UT)p were incubated with (+) or without (−) 1 pmol *M. smegmatis* UDG for 30 min and analyzed on 15% acrylamide/8 M urea gels. pd(UT)p migrates faster than pd(UT) (lane 1) due to the contribution of additional negative charges from the 3′ phosphate. Sugar-P_i and P_i are the reaction products.

Table 3. Kinetic parameters for uracil excision from the various substrates. Values shown within parentheses are for *E. coli* UDG [24] shown here with respect to SS-U9. All values are averages of at least three independent estimations. K_m values are for the uracil residues in the oligonucleotide. Ratio of V_{max}/K_m for SS-U9 set as 100%. All other values are relative to SS-U9.

Substrate	K_m	V_{max}	Relative V_{max}/K_m
	μM	pmol min^{-1} · ng $protein^{-1}$	
SS-U9	0.398 (0.33)	226 (45.7)	100 (100)
Loop-U1	0.84 (3.99)	81.9 (13.2)	17.19 (2.39)
Loop-U2	1.05 (3.99)	128 (1.52)	21.5 (0.27)
Loop-U3	0.425 (22.7)	133.9 (12.79)	55.18 (4.05)
Loop-U4	0.443 (0.252)	151.2 (17.35)	60.1 (49.8)

of the properties of *M. smegmatis* UDG, that is, its weak interaction with Ugi, and efficient utilization of the loop substrates, are in sharp contrast with those of *E. coli* (Figs 4, 5 and 10, and Table 3). Whether these properties can, in general, be attributed to UDGs from G+C-rich organisms cannot be answered at present because UDGs from no other G+C-rich organism have been characterized. An estimated molecular mass of 25 kDa for *M. smegmatis* UDG is similar to that of *E. coli* UDG and the other proteins belonging to the conserved group of UDGs [15, 34]. *M. smegmatis* UDG showed maximum activity at pH 8.0 which is also similar to that of *E. coli* UDG [26]. Both *E. coli* and *M. smegmatis* UDGs use pd(UT)p as the minimum substrate (Fig. 6; [25]). Determination of the minimum substrate size highlights that the single 5′, and the two 3′ phosphate groups of the DNA backbone flanking the uracil are essential in substrate binding to UDGs. Interestingly, the cocrystal structure of an engineered human UDG with the reaction products also showed the presence of direct hydrogen bonds between these phosphate groups and the conserved residues of UDG [35].

The N-terminal amino acid sequence of the purified *M. smegmatis* UDG begins with threonine and suggests, as in *E. coli* [22], post-translational removal of the initiator formyl-methionine. Recently, a predicted sequence of *M. tuberculosis* UDG released by the Sanger's Centre (UK) showed that its N-terminal

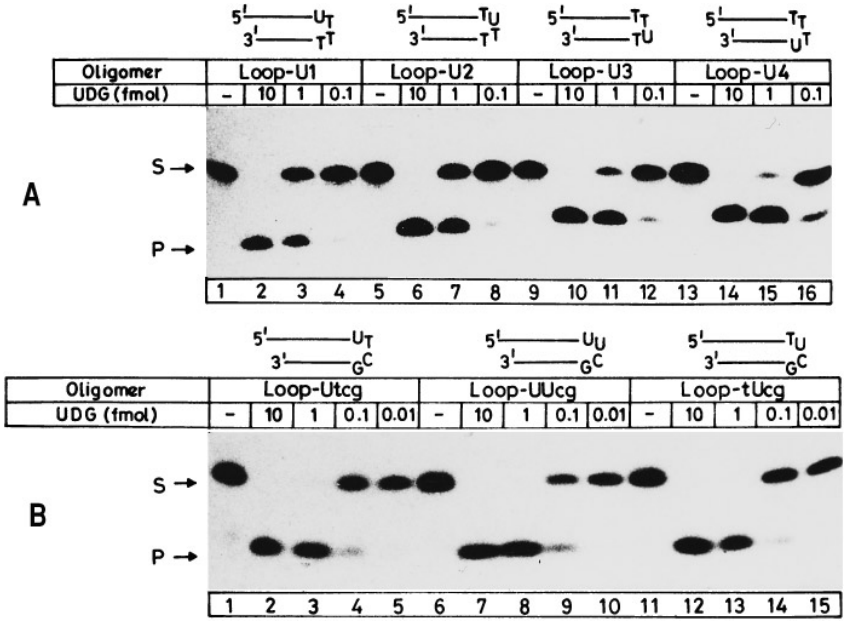

Fig. 10. Utilization of loop substrates by *M. smegmatis* UDG. 5′-end labeled oligonucleotides (2 pmol) were incubated without (−), or with 10, 1, 0.1 or 0.01 fmol *M. smegmatis* UDG under the standard UDG reaction conditions and analyzed on 8 M urea PAGE. The positions of uracil in the substrates are schematically shown above the respective lanes; S, and P indicate substrate and the product bands.

sequence, M-T-A-R-P-L-S-E-L-V-E is significantly similar to that of the *M. smegmatis* enzyme. Considering that N-terminal sequences of UDGs are not usually conserved [36], such a sequence similarity suggests that the fast growing species, *M. smegmatis* can be used as a good model system for the study of uracil excision repair pathway in mycobacteria.

Proteins belonging to the conserved group of UDGs are strongly inhibited by Ugi [32, 34]. Studies on the *E. coli* UDG-Ugi complex formation have shown that this complex is exceptionally stable, and that free Ugi does not exchange with Ugi in the formed complex [31]. Further, the human UDG is reported to be inhibited three times more efficiently than *E. coli* UDG [16]. Differential inhibition of UDGs with Ugi was also reported earlier [38, 39]. Interestingly, in this study, we show that, while the *M. smegmatis* UDG forms a complex with Ugi, the complex is dissociable and the *M. smegmatis* UDG is not efficiently inhibited by Ugi (Figs 4 and 5). Crystal structure solutions of human and HSV type-1 UDGs with Ugi have established that the two proteins interact in a 1:1 molar stoichiometry, and that Ugi acts as a DNA mimic [16, 19]. The structures also reveal a remarkable shape and charge complementarity between the two proteins and provide a basis for mutational analysis to study the mechanism of protein-protein interactions [16, 19]. Recently, mutational analysis and determination of the solution structure of the Ugi mutants in complex with *E. coli* UDG have further highlighted the significance of the various interactions between UDG and Ugi [37]. Site-specific mutants of Ugi (E20I, E27A, E28L, E30L, E31L, D61G and E78V) showed that, with the exception of E20I, all others formed a stable complex with *E. coli* UDG. The E27 and E30 positions of Ugi do not make any contacts with UDGs and, the mutations at E28, E31, E78 and D61, which make contacts with various residues in UDG [16, 19, 37], still allow formation of stable complexes. However, mutation at position E20, which led to the formation of a dissociable complex, makes two hydrogen bonds with S88 and a single hydrogen bond with P87 of *E. coli* UDG ([37], our unpublished results). Interestingly, when the sequence of *M. tuberculosis* UDG is compared with that of *E. coli*, along with certain other variations, it contained an arginine in place of Ser88. Any changes at Ser88 (or its equivalents in other UDGs) may not only result in the loss of direct contact(s) with E20 but also disrupt the contact with P87. Therefore, Ser 88 of *E. coli* UDG and its equivalents in other UDGs may well constitute one of the crucial contacts responsible for stable interaction with Ugi. These observations not only provide a rationale for the differential interaction of Ugi with *E. coli* and *M. smegmatis* UDGs, but also suggest that the latter may provide with a natural system to study the mechanism of UDG-Ugi interaction. The distinct features of *M. smegmatis* UDG also raise a possibility for the design of selective inhibitors for mycobacterial UDG [40].

Kinetics of uracil excision from different positions of a tetra T loop, where each of the loop positions was systematically substituted with dUMP, showed poor release from the second position of the loop substrates by *E. coli* UDG [24]. Further, the efficiency with which the uracil residues were excised from different loop positions varied by approximately 180-fold [24]. To our surprise, *M. smegmatis* UDG did not make a distinction between the different loop positions and the efficiency of uracil release as determined from V_{max}/K_m ratios varied only by 3−4-fold. Thus, it appears that certain details of substrate interaction to *M. smegmatis* UDG are different from those of *E. coli* UDG. However, it should be noted that many of the properties, such as the definition of the minimum substrate, requirement of the 5′-end phosphate for uracil excision from the 5′ ends, and highly inefficient release of uracil from the penultimate position of the substrates, are common both to *E. coli* and *M. smegmatis* UDGs. Hence, the structural differences may be limited to the regions not directly involved in catalysis.

This work was supported by a grant from the Department of Biotechnology, New Delhi, India. We thank Dr D. N. Rao, Ms S. Thanedar, Ms P. Handa and Ms N. Rumpal for critical reading of the manuscript and Drs I. Takahashi and H. E. Schellhorn and M. Williams to provide us with the *Bacillus subtilis* strains carrying phage PBS-1 and -2. We are grateful to Dr U. L. RajBhandary for his support in obtaining N-terminal sequence of *M. smegmatis* UDG. K. P. is a Dr K. S. Krishnan fellow (Department of Atomic Energy).

REFERENCES

1. Bloom, B. R. & Murray, C. J. L. (1992) Tuberculosis: commentary on a reemergent killer, *Science 257*, 1055−1064.
2. Kaufmann, S. H. E. & van Embden, J. D. A. (1993) Tuberculosis: a neglected disease strikes back, *Trends Microbiol. 1*, 2−5.
3. Dhandapani, S., Mudd, M. & Deretic, V. (1997) Interaction of OxyR with the promoter region of the oxyR and aphC genes from *Mycobacterium leprae* and *M. tuberculosis*, *J. Bacteriol. 179*, 2401−2409.
4. Garbe, T. R., Hibler, N. S. & Deretic, V. (1996) Response of *Mycobacterium tuberculosis* to reactive oxygen and nitrogen intermediates, *Mol. Med. 2*, 134−142.
5. Small, P. L. C., Ramkrishnan, L. & Falkow, S. (1994) Remodeling schemes of intracellular pathogens, *Science 263*, 637−639.
6. Lindahl, T. (1993) Instability and decay of the primary structure of DNA, *Nature 362*, 709−715.
7. Movahedzadeh, F., Colston, M. J. & Davis, E. O. (1997) Determination of DNA sequences required for regulated *M. tuberculosis* RecA expression in response to DNA-damaging agents suggests that two modes of regulation exist, *J. Bacteriol. 179*, 3509−3518.
8. Burgers, P. M. J. & Klein, M. B. (1986) Selection by genetic transformation of a *Saccharomyces cerevisiae* mutant defective for the nuclear Uracil-DNA glycosylase, *J. Bacteriol. 166*, 905−913.
9. Chen, J.-D. & Lacks, S. A. (1991) Role of Uracil-DNA glycosylase in mutation avoidance by *Streptococcus pneumoniae*, *J. Bacteriol. 173*, 283−290.
10. Duncan, B. K. & Weiss, B. (1982) Specific mutator effects of ung (uracil DNA glycosylase) mutations in *E. coli*, *J. Bacteriol. 151*, 750−755.
11. Fix, D. F. & Glickman, B. W. (1986) Differential enhancement of spontaneous transition mutations in the *lacI* gene of an *ung*$^-$ strain of *Escherichia coli*, *Nucleic Acids Res. 175*, 41−45.
12. Muller, S. J. & Caradonna, S. (1991) Isolation and characterization of a human cDNA encoding uracil-DNA glycosylase, *Biochim. Biophys. Acta 1088*, 197−207.
13. Gallinari, P. & Jiricny, J. (1996) A new class of uracil-DNA glycosylase related to human thymine-DNA glycosylase, *Nature 383*, 735−738.
14. Mayer-Siegler, K., Mauro, D. J., Seal, G., Wurzer, J., DeRiel, J. K. & Sirover, M. A. (1991) A human nuclear uracil DNA glycosylase is the 37 kDa subunit of glyceraldehyde-3-phosphate dehydrogenase, *Proc. Natl Acad. Sci. USA 88*, 8460−8464.
15. Krokan, H. E., Standal, R. & Slupphaug, G. (1997) DNA glycosylases in the base excision repair of DNA, *Biochem J. 325*, 1−16.
16. Mol, C. D., Aravai, A. S., Sanderson, R. J., Slupphaugh, G., Kavli, B., Krokan, H. E., Mosbaugh, D. W. & Tainer, J. A. (1995) Crystal structure of human UDG in complex with a protein inhibitor: protein mimicry of DNA, *Cell 82*, 701−708.
17. Mol, C. D., Arvai, A. S., Slupphaug, G., Kavli, B., Alseth, I., Krokan, H. E. & Tainer, J. A. (1995) Crystal structure and mutation analysis of human uracil-DNA glycosylase: structural basis for specificity and catalysis, *Cell 80*, 869−878.
18. Savva, R., McAuley-Hecht, K., Brown, T. & Pearl, L. (1995) The structural basis of specific base excision repair by uracil-DNA glycosylase, *Nature 373*, 487−493.
19. Savva, R. & Pearl, L. H. (1995) Nucleotide mimicry in the crystal structure of the uracil DNA glycosylase-uracil DNA glycosylase inhibitor protein complex, *Nat. Struct. Biol. 2*, 752−757.

20. Nagaraja, V. & Gopinathan, K. P. (1980). Requirement of calcium ions in mycobacteriophage I3 DNA infection and propagation, *Arch. Microbiol. 124*, 249−254.
21. Sambrook, J., Fritsch, E. F. & Maniatis, T. (1989) *Molecular cloning: a laboratory manual*, 2nd edn, Cold Spring Harbor Laboratory, Cold Spring Harbor, NY.
22. Varshney, U., Hutcheon, T. & van de Sande, J. H. (1988) Sequence analysis, expression, and conservation of *Escherichia coli* uracil DNA glycosylase and its gene (*ung*), *J. Biol. Chem. 263*, 7776−7784.
23. Wang, Z., Smith, D. G. & Mosbaugh, D. W. (1991) Overproduction and characterization of the uracil-DNA glycosylase inhibitor of bacteriophage PBS2, *Gene* (*Amst.*) *99*, 31−37.
24. Kumar, N. V. & Varshney, U. (1997) Contrasting effects of single stranded DNA binding protein on the activity of uracil DNA glycosylase from *Escherichia coli* towards different DNA substrates, *Nucleic Acids Res. 25*, 2336−2343.
25. Varshney, U. & van de Sande, J. H. (1991) Specificities and kinetics of uracil excision from uracil-containing DNA oligomers by *Escherichia coli* uracil DNA glycosylase, *Biochemistry 30*, 4055−4061.
26. Lindahl, T., Ljungquist, S., Siegert, W., Nybert, B. & Sperens, B. (1977) DNA N-glycosidase, properties of uracil-DNA glycosylase from *E. coli*, *J. Biol. Chem. 252*, 3286−3294.
27. Laemmli, U. K. (1970) Cleavage of structural proteins during the assembly of the head of bacteriophage T4, *Nature 227*, 680−685.
28. Towbin, H., Staehelin, T. & Gordon, J. (1979) Electrophoretic transfer of proteins from polyacrylamide gels to nitrocellulose sheets: procedures and some applications, *Proc. Natl Acad. Sci. USA 76*, 4350−4354.
29. Kumar, N. V. & Varshney, U. (1994) Inefficient excision of uracil from loop regions of DNA oligomers by *E. coli* uracil DNA glycosylase, *Nucleic Acids Res. 22*, 3737−3741.
30. Sedmak, J. J. & Grossberg, S. E. (1977) A rapid, sensitive and versatile assay for protein using Coomassie brilliant blue G250, *Anal. Biochem. 79*, 544−552.
31. Bennett, S. E., Schimerlik, M. I. & Mosbaugh, D. W. (1993) Kinetics of the uracil-DNA glycosyalse/inhibitor protein association: ung interaction with ugi, nucleic acids and uracil compounds, *J. Biol. Chem. 268*, 26879−26885.
32. Karan, P., Cone, R. & Friedberg, E. C. (1981) Specificity of the bacteriophage PBS2 induced inhibitor of uracil-DNA glycosylase, *Biochemistry 20*, 6092−6096.
33. Kumar, N. V. & Varshney, U. (1994) Excision of uracil from the ends of double stranded DNA by uracil DNA glycosylase and its use in high efficiency cloning of PCR products, *Curr. Sci. 67*, 728−734.
34. Mosbaugh, D. W. & Bennett, S. E. (1994) Uracil excision repair, *Prog. Nucleic Acid Res. Mol. Biol. 48*, 315−369.
35. Slupphaug, G., Mol, C. D., Kavli, B., Arvai, A. S., Krokan, H. E. & Tainer, J. A. (1996) A nucleotide-flipping mechanism from the structure of human uracil-DNA glycosylase bound to DNA, *Nature 384*, 87−92.
36. Sakumi, K. & Sekiguchi, M. (1990) Structures and functions of DNA glycosylases, *Mutat. Res. 236*, 161−172.
37. Lundquist, A. J., Beger, R. D., Bennett, S. E., Bolton, P. H. & Mosbaugh, D. W. (1997) Site-directed mutagenesis and characterisation of uracil-DNA glycosylase inhibitor protein, *J. Biol. Chem. 272*, 21408−21419.
38. Williams, M. V. & Pollack, J. D. (1990) A mollicute (Mycoplasma) DNA repair enzyme: purification and characterization of uracil-DNA glycosylase, *J. Bacteriol. 172*, 2979−2985.
39. Winters, T. A. & Williams, M. V. (1990) Use of the PBS2 UDG inhibitor to differentiate the uracil-DNA glycosylase activities encoded by herpes-simplex virus type 1 and 2, *J. Virol. Methods 29*, 233−242.
40. Focher, F., Verri, A., Spadari, S., Manservigi, R., Gambino, J. & Wright, G. E. (1993) Herpes simplex virus type 1 uracil-DNA glycosylase: isolation and selective inhibition by novel uracil derivatives, *Biochem. J. 292*, 883−889.